

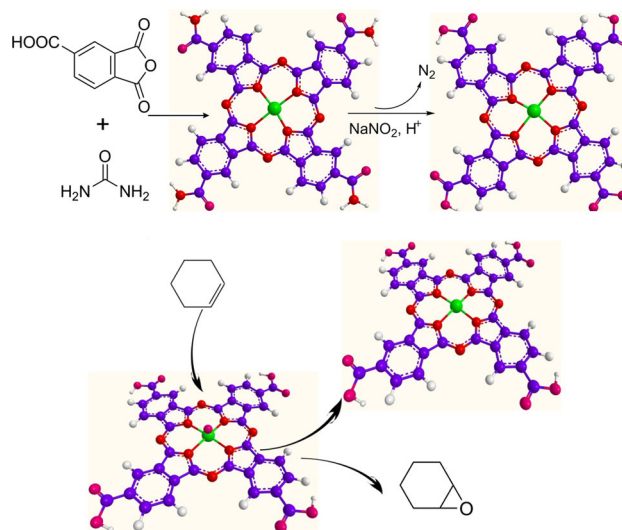
Improved Synthesis of Soluble Metal-Free/Metal Phthalocyanine Tetracarboxylic Acids and Their Application in the Catalytic Epoxidation of Cyclohexene

Xiaoling Sun · Li Wang · Zhi Tan

Received: 19 December 2014 / Accepted: 8 February 2015 / Published online: 14 February 2015
© Springer Science+Business Media New York 2015

Abstract Soluble metal-free and metal (copper (II), iron (III), and cobalt (II)) phthalocyanine tetracarboxylic acids (**5–8**) were synthesized using a novel method consisting of improved hydrolysis based on the diazo reaction. The obtained compounds (**5–8**) were characterized by X-ray diffraction, UV–Vis spectrometry, and FT-IR spectrometry and then utilized as catalysts for the epoxidation of cyclohexene with molecular oxygen as oxidant. Reaction conditions including reaction time, temperature, catalyst amount, and isobutyraldehyde/cyclohexene ratio were optimized to achieve the highest selectivity of cyclohexene oxide. Metal-free phthalocyanine tetracarboxylic acid (**5**) and metal (copper (II), iron (III), and cobalt (II)) phthalocyanine tetracarboxylic acids (**6–8**, respectively) were compared. Complexes **6–8** exhibited higher catalytic activity than compound **5** under the optimal conditions.

Graphical Abstract Four soluble metal-free and metal PTCs were synthesized using a novel method, and were utilized as catalysts for the epoxidation of cyclohexene with molecular oxygen as the oxidant. A total of 58.1% selectivity and yield of cyclohexene oxide were achieved under the optimal condition.



Keywords Metal-free phthalocyanine · Metal phthalocyanine · Epoxidation · Cyclohexene · Molecular oxygen

1 Introduction

Phthalocyanine derivatives have been traditionally used as pigments and dyes [1, 2]. Scholars found that phthalocyanines exhibit unique optical, physical, chemical, and catalytic properties because of their extensively delocalized 18 π -electron aromatic heterocyclic system [3]. As a result, phthalocyanines have been utilized as catalysts [4, 5], chemical sensors [6, 7], solar cells [8–10], and photodynamic therapy materials [11, 12]. However, phthalocyanines exhibit poor solubility and can only be dissolved in

X. Sun (✉) · L. Wang · Z. Tan
School of Chemical and Environmental Engineering, Shanghai
Institute of Technology, Shanghai 201418, China
e-mail: xiaolingsun1@msn.com

concentrated sulfuric acid or strong polar solvents, such as DMF, DMSO, pyridine, and THF [13]; hence, the use of phthalocyanines as catalysts in various catalytic reactions has been significantly limited. Therefore, water-soluble phthalocyanine derivatives have been synthesized over the recent years to improve their catalytic properties [14–16]. Soluble phthalocyanines are usually substituted with ionic-type or strong polar hydrophilic groups, such as carboxyl, sulfonic, and ammonium groups [17, 18]. Soluble phthalocyanines are also related to the pH of the solvent [19].

Phthalocyanines have been traditionally prepared through phthalic anhydride method [20], which can be divided into two parts: solid state and liquid phase. The liquid-phase method uses toxic solvents, such as nitrobenzene and trichlorobenzene [21]. In this process, the solvent is recycled, thus causing difficulty in separating the product. The solid-phase method is a simple process and does not cause pollution and does not recycle solvents. In this paper, metal-free and metal phthalocyanine tetracarboxylic acid compounds (PTCs) were synthesized using the solid-phase method. Traditionally, metal-free and metal phthalocyanine tetraformamido compounds are initially synthesized [22] and then hydrolyzed to obtain metal-free and metal PTCs. However, metal-free and metal phthalocyanine tetraformamido compounds exhibit alkali resistance, heat resistance, water resistance, lightfastness, and insolubility in various polar and non-polar organic solvents. Therefore, strong acids and bases must be used for the hydrolysis of metal-free and metal phthalocyanine tetraformamido compounds at a high temperature with a reaction time of 12 or even 24 h [23]. For this reason, we improved the hydrolysis process based on the diazo reaction; metal-free and metal phthalocyanine tetraformamido compounds are dissolved in sulfuric acid solution, reacted with sodium nitrite solution, and then subjected to acidizing to obtain purified metal-free and metal PTCs. In this method, the hydrolysis process changes from a heterogeneous to a homogeneous reaction, thus easily reacting at room temperature and significantly reducing the reaction time from 12 or 24 h to 0.5–3 h. The improved method presents high efficiency and low cost and produces products with abundant color and high purity.

The epoxidation of cyclohexene to cyclohexene oxide is an important procedure in chemical and pharmaceutical industries because the latter is a key intermediate in organic synthesis of fine chemicals [24, 25]. Many efficient catalysts, such as nanocrystalline mesoporous TiO_2 loaded with RuO_2 [26], porous titanasilicate composite [27], and zirconium phenylphosphonate-anchored methyltrioxorhenium [28], have been used for the epoxidation of cyclohexene with H_2O_2 as the oxidant. Although hydrogen peroxide exhibits advantages compared with other conventional epoxidants, such as PhIO , NaClO , and $t\text{-BuOOH}$ [29], molecular oxygen

has gained significant attention because it is a cheap, environmentally clean, and readily available oxidant since 1990s. Mukaiyama first reported epoxidation of olefins catalyzed by nickel (II) complexes with combined use of oxygen and aldehydes [30], then Iqbal explored the epoxidation with methyl-2-oxocyclopentane carboxylate in the presence of the cobalt (II) catalyst and oxygen [31]. Moreover, Iqbal et al. [32] reviewed a lot of transition metal complexes as catalyst for epoxidation of olefins with molecular oxygen. Thus, in this paper, metal-free and metal PTCs were used as catalysts for the epoxidation of cyclohexene with molecular oxygen and isobutyraldehyde at room temperature and atmospheric pressure.

In this study, we synthesized metal-free PTC (5) through the improved method first, which could be regarded as a ligand for its unique central structure. Then we prepared metal PTCs (6–8) by adding anhydrous metal salts (CoCl_2 , CuSO_4 , and FeCl_3) during the preparation of compound 5. All of these compounds were characterized through IR, UV spectrometry, and XRD. Catalytic activities of compounds 5–8 were also screened using the epoxidation of cyclohexene with molecular oxygen as the oxidant under mild conditions. The effects of different experimental parameters, including reaction time, temperature, catalyst amount, and isobutyraldehyde/cyclohexene ratio, were further investigated to optimize the reaction conditions.

2 Experimental

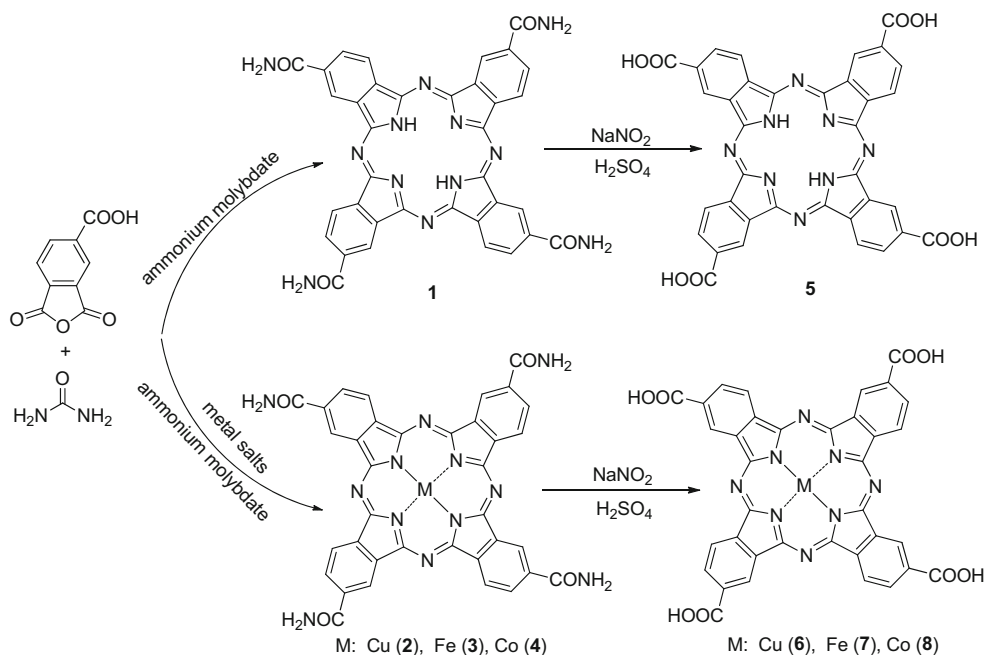
2.1 Materials

All solvents and chemicals were of analytical grade, obtained from commercial suppliers, and used without purification unless otherwise stated.

2.2 Preparation of Metal-Free and Metal PTCs (5–8)

Scheme 1 presents the synthesis pathway of metal-free and metal PTCs (5–8). Trimellitic anhydride (50 mmol), urea (0.5 mol), and ammonium molybdate (0.1 mmol) as catalyst were used for preparation. For metal PTCs (6–8), equivalent amounts (50 mmol) of the corresponding anhydrous metal salts (CoCl_2 , CuSO_4 , and FeCl_3) were placed into a three-necked flask with a reflux condenser. After grinding and blending, the reaction mixture was stirred at 170 °C for 6 h and then cooled to room temperature. The resulting mixture was boiled in 5 mol/L hydrochloric acid and then filtered. The mixture was simultaneously washed with anhydrous ether and absolute methanol until the filtrate became colorless. Metal-free and metal phthalocyanine tetraformamido compounds (1–4) were obtained. Compounds 1–4 were dissolved in 50 %

Scheme 1 Synthesis of metal-free and metal phthalocyanine tetracarboxylic acid complexes



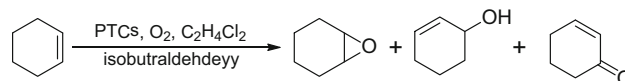
sulfuric acid solution (170 mL) and added with 2 mol/L sodium nitrite solution (14 mL) drop wise while stirring at 5 °C. The reaction mixture was maintained at 30 °C for 1 h with constant stirring. The solvent was removed through centrifugal separation and filtration, and the resulting solid was dissolved in deionized water. The resulting solution was neutralized with 2 mol/L H_2SO_4 solution to obtain a pH of 3. The solution was then filtered after standing for 12 h. The resulting solid was dried in a vacuum oven after washing. The temperature was maintained at 70 °C and the vacuum degree at 0.07 MPa for 4 h. Compounds **5–8** were obtained with a yield of 2.5 (26.9 %), 1.85 (19.8 %), 2.1 (22.5 %), and 2.5 g (26.9 %), respectively.

2.3 Characterization

Compounds **5–8** were characterized through X-ray diffraction, diffuse reflectance UV–Vis, and FT-IR. FT-IR spectrum was performed on a Thermo Nicolet Nexus Magana-IR500 FT-IR spectrometer with the standard KBr pellet method. Compounds **5–8** were dissolved in solvents and put it into quartz cell (10 mm) to detect the UV–Vis spectra by Shimadzu UV-3600 spectrophotometer. Powder X-ray diffraction was performed on an X'Pert PRO diffractometer using Cu $\text{K}\alpha$ ($\lambda = 0.0016711$ nm) radiation operating at 40 kV and 40 mA with the scanning 2θ range from 0° to 90°.

2.4 Catalytic Activity Measurement

The general procedure for the epoxidation of cyclohexene was presented as follows (Scheme 2). 1, 2-Dichloroethane



Scheme 2 Epoxidation of cyclohexene catalyzed by PTCs

(10 mL), isobutyraldehyde (0.048 mol), cyclohexene (0.024 mol), and a catalyst (3 % of the mass fraction of cyclohexene) were placed into a three-necked flask with a reflux condenser. The resulting mixture was stirred by bubbling molecular oxygen at 35 °C for 10 h. After centrifugal separation, the resulting solution was analyzed through GC and GC–MS for qualitative and quantitative analyses.

3 Results and Discussion

3.1 FT-IR Absorption Spectra

Figure 1 illustrates the comparison of the FT-IR absorption spectra. The results of the FT-IR spectra of compounds **5–8** are presented in Table 1. Compounds **5–8** featured a carboxyl group and showed the characteristic $\text{C}=\text{O}$ band at 1711–1717 cm^{-1} [33] and $\text{O}-\text{H}$ band at 3425–3450 cm^{-1} in the IR spectrum. The peaks of compounds **5–8** around 1276–1286 cm^{-1} were attributed to the $\text{C}-\text{N}=\text{C}$ stretching vibration, whereas the peaks around 1146–1151, 1084–1092, 1055–1065, 938–944, and 735–741 cm^{-1} were due to phthalocyanine skeletal vibrations [34]. The peak around 1420–1421 cm^{-1} showed that aromatic phenyl ring existed in the compounds (**5–8**). The fluctuation range of

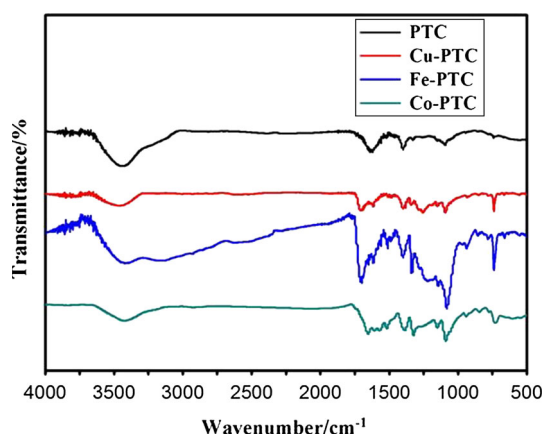


Fig. 1 The FT-IR spectrum of metal-free and metal phthalocyanine tetracarboxylic acid compounds

the peaks may be caused by the electron-withdrawing ability of metal cations. These data showed that compounds **5–8** exhibited the carbon skeleton structure of phthalocyanine and carboxyl groups.

3.2 UV-Vis Absorption Spectra

The UV-Vis spectra of phthalocyanines mainly originated from $\pi \rightarrow \pi^*$ transitions of the strong Q-band (600–750 nm) and the broad B-band (300–450 nm) with weak transitions near those bands [35–38]. Compounds **5–8** were dissolved in DMSO before UV-Vis analysis, and their UV-Vis spectra are shown in Fig. 2. The resulting absorption wavelength in Table 2 demonstrated that all compounds (**5–8**) exhibited a similar specific absorption peak of the phthalocyanine aromatic ring. The comparison of the absorption wavelength showed that the UV-Vis spectrum of compound **5** exhibited stronger Q-band absorptions at $\lambda_{\max} = 699$ nm than the absorptions of complexes **6–8** at $\lambda_{\max} = 686, 664,$ and 675.2 nm, respectively. This phenomenon could be attributed to the substitution of the central hydrogen atoms of metal-free PTC by metal atoms, thus significantly reducing the electron cloud density of the metal-free PTC ring and increasing the energy level between HOMO and LUMO. Therefore, the absorptions demonstrated a blue shift.

The UV-Vis spectra of metal PTCs were not only affected by central metal atoms and substituent groups, but

also by solvent concentration and types of solvents. Hence, the UV-Vis spectra of Co-PTC were detected in DMSO at concentrations of $2 \times 10^{-6}, 4 \times 10^{-6}, 6 \times 10^{-6},$ and 8×10^{-6} M. Figure 3 shows that the absorbance of Co-PTC at B and Q bands increased with increasing DMSO concentration. Otherwise, the absorbance of Co-PTC in DMSO and DMF at the same concentration of 2×10^{-6} M were also detected (Fig. 4). Co-PTC in DMSO showed stronger absorbance at B and Q bands than that in DMF, and the maximum absorbance peak demonstrated a weak blue shift.

3.3 X-ray Diffraction

The XRD patterns of compounds **5–8** are presented in Fig. 5; at 2θ , two characteristic diffraction peaks, namely, a broad peak around 5.5° and a sharp peak around 27° , were observed [39, 40]. The strength of small diffraction peaks at 5.5° was weak, whereas the large diffraction peaks at 27° was strong. Table 3 shows the main peaks of PTCs as follows: metal-free PTCs at 2θ of 5.5° and 26.8° , Cu-PTC at 2θ of 5.4° and 27.1° , Fe-PTC at 2θ of 5.6° and 26.9° , and Co-PTC at 2θ of 5.7° and 27.0° . The relatively small differences in the XRD patterns of compounds **5–8** may be attributed to the different central atoms; the peak of complex **5** at wide angle was smaller than the peaks of complexes **6–8**. Moreover, compounds **5–8** exhibited similar crystalline structure.

3.4 Catalytic Activity

3.4.1 Effect of Reaction Time on the Epoxidation of Cyclohexene

The effect of reaction time was initially studied within 2–10 h, and the results are shown in Table 4. The yield and conversion to cyclohexene oxide drastically increased with the increasing reaction time from 2 to 8 h. However, the isomerization of cyclohexene oxide to olefin aldehyde occurred when the reaction time was prolonged to 10 h, thus decreasing the selectivity. This finding showed that 8 h was the optimum reaction time to obtain the highest cyclohexene oxide conversion and selectivity.

Table 1 The FT-IR spectrum of metal-free and metal phthalocyanine tetracarboxylic acid compounds

PTCs	FT-IR (cm^{-1})
PTC (5)	3425, 1685, 13439, 1717, 1421, 1284, 1151, 1092, 1063, 944, 862, 741
Cu-PTC (6)	3450, 1715, 1420, 1286, 1148, 1092, 1055, 938, 855, 739
Fe-PTC (7)	3425, 1711, 1421, 1280, 1146, 1084, 1065, 942, 856, 739
Co-PTC (8)	3426, 1717, 1420, 1276, 1150, 1091, 1058, 942, 846, 735

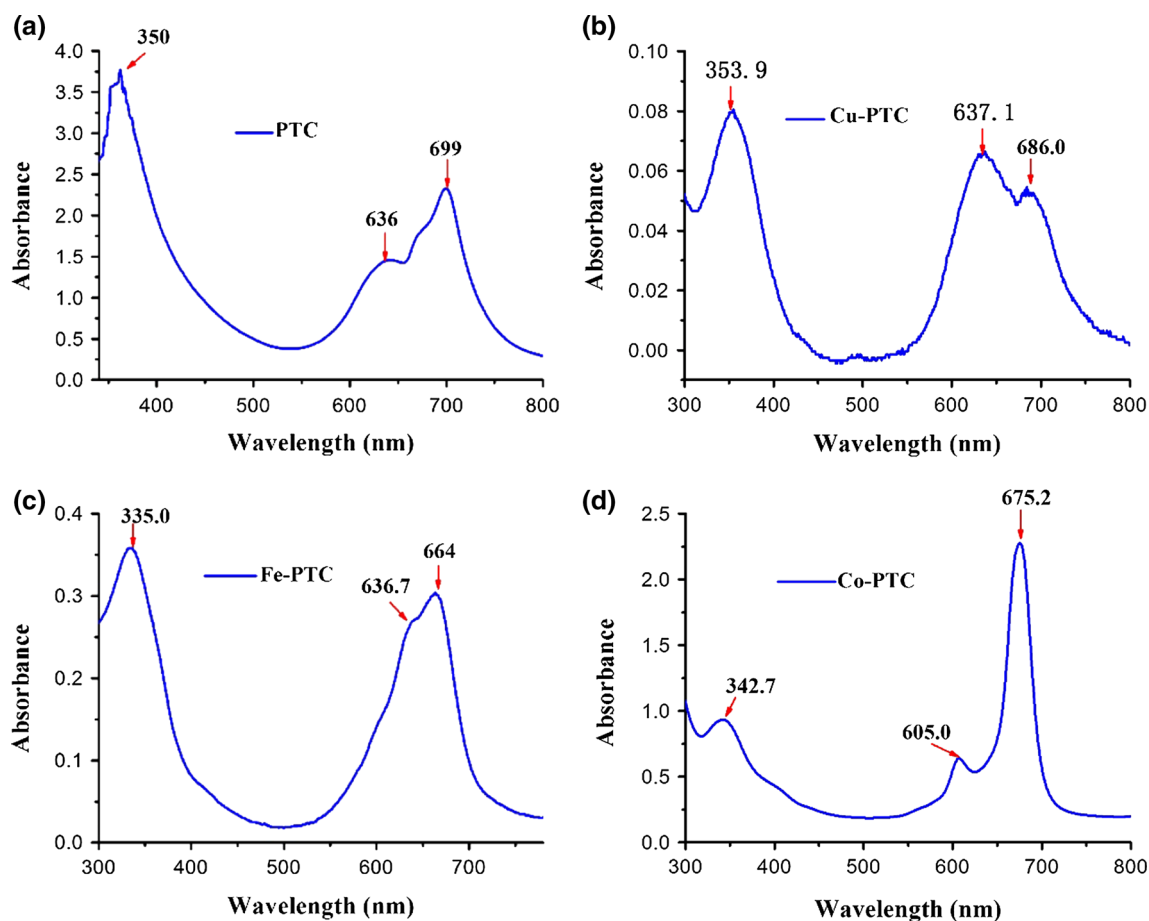


Fig. 2 Absorption spectra of PTCs in DMSO at the concentration of 4×10^{-5} M for **a** compound **5**, **b** complex **6**, **c** complex **7**, and **d** for complex **8**

Table 2 The UV-Vis spectrum of metal-free and metal phthalocyanine tetracarboxylic acid compounds

PTCs	B-band (nm)	Q-band (nm)
PTC (5)	350.0	636.0, 699.0
Cu-PTC (6)	353.9	637.1, 686.0
Fe-PTC (7)	335.0	636.7, 664.0
Co-PTC (8)	342.7	605.0, 675.2

3.4.2 Effect of Reaction Temperature on the Epoxidation of Cyclohexene

The temperature was optimized by maintaining the reaction time at 8 h, and the effects of reaction temperature are shown in Table 5. The selectivity and yield of cyclohexene increased with increasing temperature, peaked at 35 °C, and then gradually declined. Cyclohexene oxide may be easily isomerized at a high temperature. Therefore, the reaction temperature of 35 °C provided the highest cyclohexene conversion and selectivity.

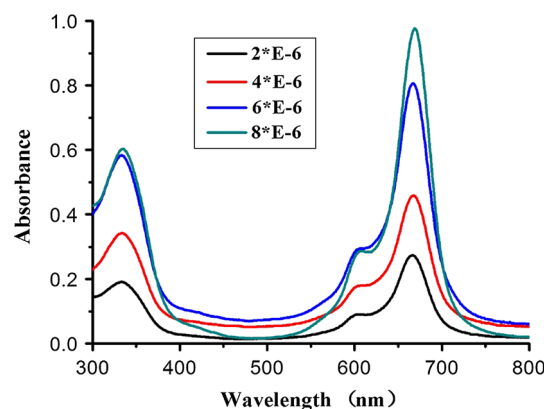


Fig. 3 Absorption spectra of Co-PTC in DMSO at the concentration of 2×10^{-6} to 8×10^{-6} M

3.4.3 Effect of Catalyst Amount on the Epoxidation of Cyclohexene

The catalyst amount was also optimized, and the results are shown in Table 6. The highest yield of cyclohexene oxide

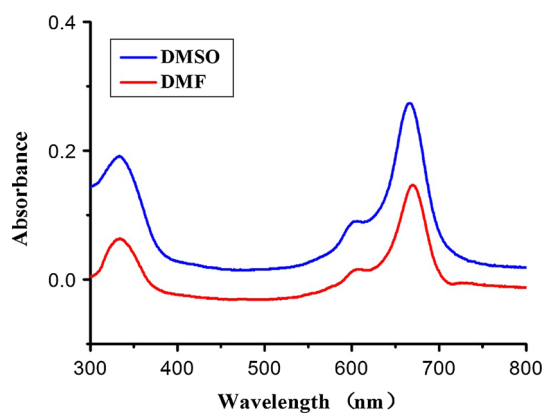


Fig. 4 Absorption spectra of Co-PTC in DMSO and DMF at the concentration of 2×10^{-6} M

was 58.1 % with increasing catalyst amount. However, the yield of cyclohexene oxide declined when the catalyst amount was further increased. By considering the selectivity of cyclohexene oxide and the conversion of cyclohexene, the catalyst amount of 0.06 g was selected under identical reaction conditions.

3.4.4 Effect of Isobutyraldehyde Amount on the Epoxidation of Cyclohexene

The amount of isobutyraldehyde was another parameter that influenced the yield of cyclohexene oxide and thus should be further optimized. The cyclohexene amount was set as constant to determine the effect of isobutyraldehyde amount over a wide range of isobutyraldehyde to cyclohexene molar ratios from 1 to 4. The results are listed in Table 7. Table 7 illustrates the selectivity and yield of cyclohexene oxide in relation to the isobutyraldehyde/cyclohexene ratio. The selectivity of cyclohexene oxide

Table 3 The X-ray diffraction patterns of metal phthalocyanine tetracarboxylic acid compounds

PTCs	2θ ($^\circ$)	
PTC (5)	5.5	26.8
Cu-PTC (6)	5.4	27.1
Fe-PTC (7)	5.6	26.9
Co-PTC (8)	5.7	27.0

Table 4 Reaction time factor of epoxidation of cyclohexene

Time (h)	Selectivity (%)	Conversion (%)	Yield (%)
2	52.0	33.30	17.3
4	49.6	76.80	38.1
6	50.0	95.4	47.7
8	48.8	100.0	48.8
10	23.4	100.0	23.4

Reaction conditions: 0.02 mol cyclohexene, 0.04 mol isobutyraldehyde, 0.06 g Co-PTC, 30 mL/min O_2 , 10 mL dichloroethane, 35 $^\circ C$

Table 5 Reaction temperature factor of epoxidation of cyclohexene

Temperature ($^\circ C$)	Selectivity (%)	Conversion (%)	Yield (%)
25	41.3	100.0	41.3
30	45.7	100.0	45.7
35	50.1	100.0	50.1
40	44.6	100.0	44.6
45	35.9	100.0	35.9

Reaction conditions: 0.02 mol cyclohexene, 0.04 mol isobutyraldehyde, 0.06 g Co-PTC, 30 mL/min O_2 , 10 mL dichloroethane, 8 h

easily reached 58.1 % when the isobutyraldehyde/cyclohexene ratio was equal to 2. However, the selectivity of cyclohexene oxide increased at isobutyraldehyde/cyclohexene ratios higher than 2. Therefore, the isobutyraldehyde/cyclohexene ratio of 2 was selected as the optimal amount for the epoxidation of cyclohexene.

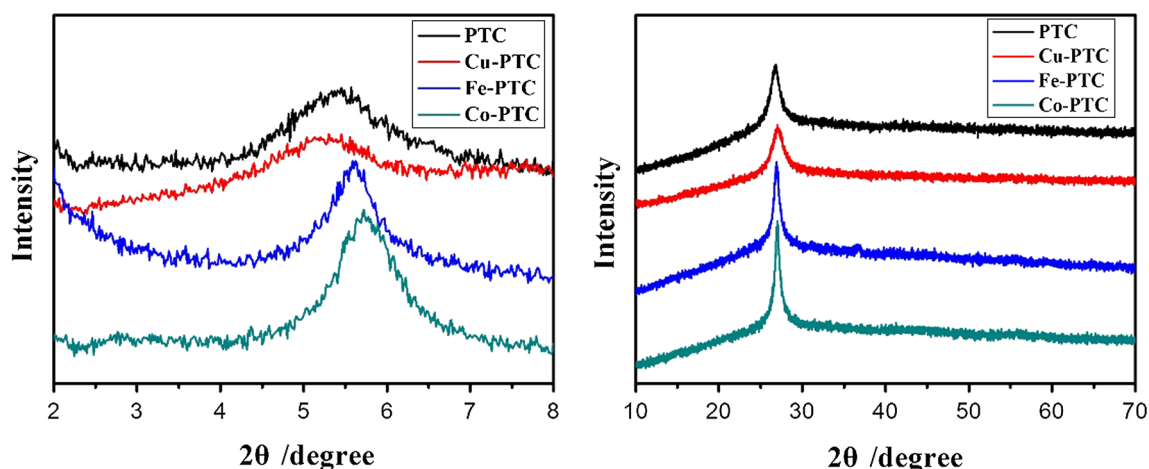


Fig. 5 The X-ray diffraction patterns of PTCs

Table 6 The influence of catalyst amount

Catalyst (g)	Selectivity (%)	Conversion (%)	Yield (%)
0.00	61.2	21.56	13.2
0.02	48.4	89.20	43.2
0.04	55.0	92.20	50.7
0.06	58.1	100.0	58.1
0.08	23.9	98.0	23.4

Reaction conditions: 0.02 mol cyclohexene, 0.04 mol isobutyraldehyde, 30 mL/min O₂, 10 mL dichloroethane, 35 °C, 8 h

Table 7 The influence of isobutyraldehyde amount

Isobutyraldehyde/ cyclohexene ratios	Selectivity (%)	Conversion (%)	Yield (%)
1	33.2	100.0	33.2
2	58.1	100.0	58.1
3	56.1	100.0	56.1
4	48.7	100.0	48.7

Reaction conditions: 0.02 mol cyclohexene, 0.06 g Co-PTC, 30 mL/min O₂, 10 mL dichloroethane, 35 °C, 8 h

Table 8 Epoxidation of cyclohexene by different complexes

Complex	Selectivity (%)	Conversion (%)	Yield (%)
5	43.0	70.3	30.2
6	55.6	90.0	50.0
7	57.6	97.4	56.1
8	58.1	100.0	58.1

Reaction conditions: 0.02 mol cyclohexene, 0.04 mol isobutyraldehyde, 0.06 g complex, 30 mL/min O₂, 10 mL dichloroethane, 35 °C, 8 h

3.4.5 Catalytic Activity of Compounds 5–8

The results of catalytic activity of compounds 5–8 are listed in Table 8. Table 8 shows that metal PTCs 6–8 exhibited high catalytic activity with the yield of cyclohexene oxide ranging from 50.0 to 58.1 %. By using metal-free PTC 5 as the catalyst for the reaction, only 30.2 % of cyclohexene oxide yield was obtained. Therefore, the catalytic activity of complexes 6–8 was higher than compound 5.

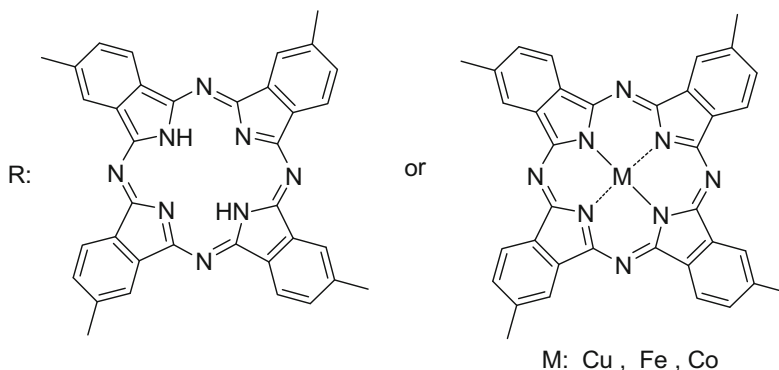
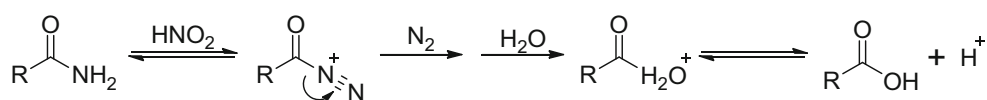
All compounds (5–8) are promising catalysts with a high catalytic activity for the epoxidation of cyclohexene under the optimal reaction conditions. The recyclability of the catalyst must be further evaluated.

3.5 Mechanistic Studies

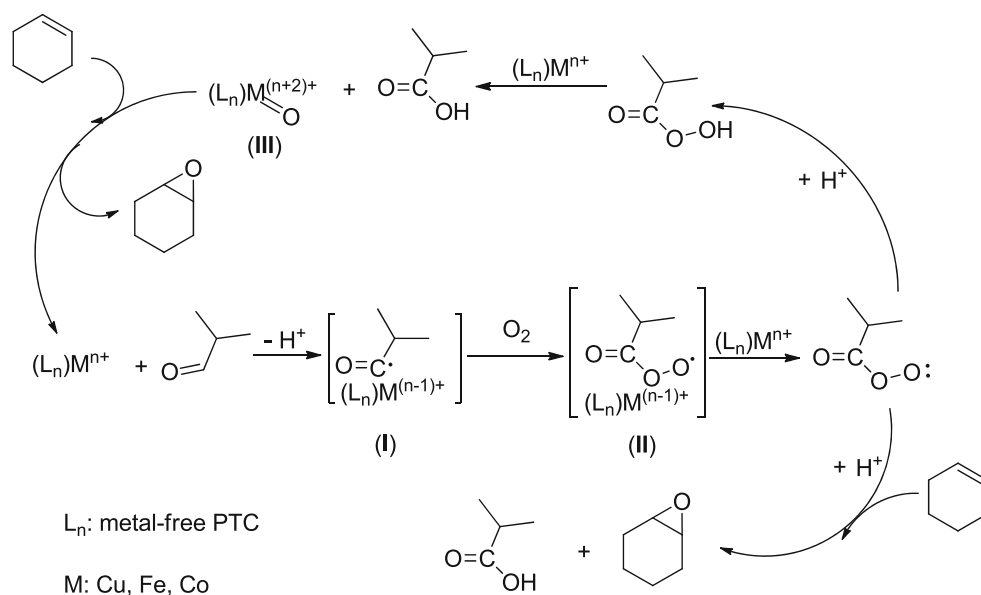
The possible mechanism of hydrolysis is illustrated in Scheme 3. was obtained through the reaction of HONO and –NH₂·N₂ was generated through the decomposition of when heated. The acyl cation was also generated; this cation immediately combined with the nucleophilic water molecule. Carboxylic acid was obtained by losing a proton.

We hold the opinion that the reaction mechanism of metal PTCs catalyze epoxidation of cyclohexene with molecular oxygen and isobutyraldehyde is similar to the published reports [41, 42] which is illustrated in Scheme 4. First, isobutyraldehyde adsorptions on the central of (L_n)-Mⁿ⁺ to generate acyl radical with a proton left and the reduction of Mⁿ⁺ to M⁽ⁿ⁻¹⁾⁺, then intermediate complex species (I) is formed. Second, molecular oxygen adsorptions on intermediate complex species (I) to generate intermediate complex species (II) which is unstable for its structure, then acylperoxy radical released immediately from intermediate complex species (II) with (L_n)Mⁿ⁺

Scheme 3 Hydrolysis mechanism of metal-free and metal phthalocyanine tetraformamido complexes



Scheme 4 The reaction mechanism for the epoxidation of cyclohexene catalyzed by PTCs



regenerated. Third, acylperoxy radical receives a proton to form isobutyryl-peroxyacid. On one hand, isobutyryl-peroxyacid reacts with cyclohexene directly to obtain cyclohexene oxide and isobutyric acid as a reaction by-product; on the other hand, isobutyryl-peroxyacid adsorptions on the central of $(L_n)M^{n+}$ and transfers an oxygen atom to $(L_n)M^{n+}$, which may generate an oxometallic active species **(III)** [43] and isobutyric acid as by-product. At last, oxometallic active species **(III)** reacts with cyclohexene to generate cyclohexene oxide, and the $(L_n)M^{n+}$ regenerated at the same time.

4 Conclusions

Four soluble metal-free and metal PTCs (**5–8**) were synthesized using a novel method. The characterization of the compounds (**5–8**) through IR spectra, UV–Vis spectra, and X-ray diffraction confirmed the existence of the phthalocyanine skeleton and the carboxyl group. Compounds **5–8** were also utilized as catalysts for the epoxidation of cyclohexene with molecular oxygen as the oxidant. Reaction conditions including reaction time, temperature, catalyst amount, and isobutyraldehyde/cyclohexene ratio were optimized to achieve the highest selectivity and yield of cyclohexene oxide. A total of 58.1 % selectivity and yield of cyclohexene oxide were achieved under the optimal condition consisting of a reaction time, temperature, isobutyraldehyde/cyclohexene ratio, and catalyst amount of 8 h, 35 °C, 2 and 0.06 g, respectively.

Acknowledgments The work was supported by the Shanghai Natural Science Foundation (No. 4ZR1440900) and Shanghai Alliance

Program (No. LM201336). The authors thank the Analysis and Testing Center of Shanghai Institute of Technology for support.

References

- Liu AZ, Lei SB (2007) *Surf Interface Anal* 39:33
- Moons H, Łapok Ł, Loas A, Van Doorslaer S, Gorun SM (2010) *Inorg Chem* 49:8779
- Sakamoto K, Ohno-Okumura E (2009) *Materials* 2:1127
- Lu WY, Li N, Chen WX, Yao YY (2009) *Carbon* 47:3337
- Chen WX, Lu WY, Yao YY, Xu MH (2007) *Environ Sci Technol* 41:6240
- Shu JH, Wickle HC, Chin BA (2010) *Sens Actuator B Chem* 148:498
- Wu WT, Wu WH, Ji SM, Guo HM, Wang X, Zhao JZ (2011) *Dyes Pigm* 89:199
- Kimura M, Nomoto H, Suzuki H, Ikeuchi T, Matsuzaki H, Murakami TN, Furube A, Masaki N, Griffith MJ, Mori S (2013) *Chem A Eur J* 19:7496
- Zhang MJ, Lv JY, Pan QJ, Guo YR (2014) *Theor Chem Acc* 133:1582
- Matsuzaki H, Murakami TN, Masaki N, Furube A, Kimura M, Mori S (2014) *J Phys Chem C* 118:17205
- Demirbaş Ü, Bayrak R, Pişkin M, Akçay HT, Durmuş M, Kantekin H (2013) *J Organomet Chem* 724:225
- Zheng BY, Zhang HP, Ke MR, Huang JD (2013) *Dyes Pigm* 99:185
- Bayrak R, Akçay HT, Beriş FŞ, Şahin E, Bayrak H, Demirbaş Ü (2014) *Spectrochim Acta A* 133:272
- Çakır V, Çakır D, Pişkin M, Durmuş M, Bıyıklıoğlu Z (2014) *J Lumin* 154:274
- Nabid MR, Asadi S, Shamsianpour M, Sedghi R, Osati S, Safari N (2010) *React Funct Polym* 70:75
- Nabid MR, Sedghi R, Jamaat PR, Safari N, Entezami AA (2007) *Appl Catal A Gen* 328:52
- Bayır ZA (2005) *Dyes Pigm* 65:235
- Sevim AM, Ilgün C, Gül A (2011) *Dyes Pigm* 89:162
- Minnes R, Weitman H, Lee HJ, Gorun SM, Ehrenberg B (2006) *Photochem Photobiol* 82:593

20. Jung KS, Kwon JH, Son SM, Shin JS, Lee GD, Park SS (2004) *Synth Met* 141:259
21. Kharisov BI, Blanco LM, Torres-Martinez LM, García-Luna A (1999) *Ind Eng Chem Res* 38:2880
22. Negri RM, Zalts A, San Román EA, Aramendía PF, Braslavsky SE (1991) *Photochem Photobiol* 53:317
23. Chen JM, Zhang JC, Shen Y, Liu XH (2000) *Proc SPIE* 4086:749
24. Ghorbanloo M, Rahmani S, Yahiro H (2013) *Transit Met Chem* 38:725
25. Peng Y, Li ZY, Tang RR (2013) *RSC Adv* 3:19965
26. Sreethawong T, Yamada Y, Kobayashi T, Yoshikawa S (2006) *J Mol Catal A Chem* 248:226
27. Jiang YQ, Li XW, Zhang SC, He YD, Li GH, Li DF, Xu XZ, Lin KF (2014) *Mater Lett* 132:270
28. He S, Liu X, Zhao HY, Zhu Y, Zhang FZ (2015) *J Colloid Interface Sci* 437:58
29. Li ZY, Tang RR, Liu GY (2013) *Catal Lett* 143:592
30. Yamada T, Takai T, Rhode O, Mukaiyama T (1991) *Chem Lett* 20:5
31. Punniyamurthy T, Bhatia B, Iqbal J (1993) *Tetrahedron Lett* 34:4657
32. Punniyamurthy T, Velusamy S, Iqbal J (2005) *Chem Rev* 105:2329
33. Sharman WM, Van Lier JE (2005) *J Porphyr Phthalocyanines* 9:651
34. Achar BN, Lokesh KS (2004) *J Solid State Chem* 177:1987
35. Nas A, Kantekin H, Durmuş M, Gümrükçüoğlu N (2014) *J Lumin* 154:15
36. Zhang XF, Lin Y, Guo WF, Zhu JZ (2014) *Spectrochim Acta A* 133:752
37. Özil M, Açar E, Şaşmaz S, Kahveci B, Akdemir N, Gümrükçüoğlu İE (2007) *Dyes Pigm* 75:732
38. Ghani F, Kristen J, Riegler H (2012) *J Chem Eng Data* 57:439
39. Li DP, Ge SX, Sun GF, He Q, Huang BJ, Tian GZ, Lu WY, Li GB, Chen YL, An SN, Zheng Z (2015) *Dyes Pigm* 113:200
40. Mani V, Devasenathipathy R, Chen SM, Gu JA, Huang ST (2015) *Renew Energy* 74:867
41. Nam W, Kim JH, Kim SH, Ho RYN, Valentine JS (1996) *Inorg Chem* 35:1045
42. Li ZY, Liu CH, Tang RR, Liu G (2013) *RSC Adv* 3:9745
43. Angelescu E, Ionescu R, Pavel OD, Zăvoianu R, Bîrjega R, Luculescu CR, Florea M, Olar R (2010) *J Mol Catal A Chem* 315:178